Autoignition and Extinction of Mixtures of Ethanol and Dimethyl Ether

A. Loukou[*1,2], J. Reiter[3,4], R. Gehmlich[3], C. Hasse[5], D.Trimis[2], E. Pucher[4], and K. Seshadri[3]

[1]Institute of Thermal Engineering, TU-Bergakademie Freiberg, Freiberg, Germany
[2]Engler-Bunte-Institute, Karlsruhe Institute of Technology, Karlsruhe, Germany
[3] Department of Mechanical and Aerospace Engineering, University of California at San Diego, La Jolla, California, USA
[4] Institute for Powertrains and Automotive Technology, Vienna University of Technology, Vienna, Austria
[5]Chair of Numerical Thermo-Fluid Dynamics, ZIK Virtuhcon, TU Bergakademie Freiberg, Freiberg, Germany

Abstract

This work is concerned with non-premixed combustion of the C_2H_6O isomers, dimethyl ether (DME) and ethanol, in non-uniform flows. Experimental studies were carried out employing the counter flow burner configuration in order to define critical conditions of extinction and autoignition for the two fuels and for different blends of them. In order to measure critical conditions of extinction the mass fractions of the reactants were selected with the aim of keeping constant the adiabatic flame temperature and the stoichiometric mixture fraction in all examined flames. The strain rate at extinction was recorded as a function of the relative amounts of DME and ethanol in the combustible mixture. In the case of autoignition, the mass fraction of fuel was fixed at 0.40 while the composition was varied, covering the pure substances and several blends. For every fuel composition, the temperature of the oxidizer stream at autoignition was recorded as function of the strain rate.

Introduction

Dimethyl ether (DME; CH_3OCH_3) and ethanol (CH_3CH_2OH) are regarded as alternative or additive fuels for the transportation sector due to their renewable nature and their potential for reducing pollutant emissions [1–4]. At the same time they are isomers of C_2H_6O and thus, there is a lot of interest in exploring differences in their combustion behavior that could result from their different chemical structures. A comparison of the thermophysical properties of the two fuels is presented in Table 1:

Table 1: Properties of DME and ethanol

Chemical Structure	CH_3-O-CH_3	CH_3-CH_2-OH
Molecular Weight (g/mol)	46.07	46.07
Carbon Content (wt%)	52.20	52.20
Cetane Number	55 – 60	-
Octane Number (RON)	-	110
Density (kg/m^3)@298 K	1.86	785
Normal Boiling Point (°C)	-24.9	78
LHV (MJ/kg)	28.62	26.87
Heat of Vaporization (kJ/kg)	467	900
Vapor Pressure [kPa]@298 K	596.21	-

Properties of premixed ethanol flames like laminar burning velocities, species profiles and soot emissions have been experimentally determined in many earlier studies (eg. [4–7]). Similarly, features of non-premixed ethanol flames like extinction, autoignition and pollutant emissions have also been addressed in previous works (e.g. [8–11]). Regarding premixed flames of DME, previous studies have dealt with measurements of laminar burning velocities and pollutant emissions (e.g. [2,12–14]). The role of the low temperature DME oxidation chemistry (NTC-regime) has been examined in few studies including premixed and non-premixed flames (e.g. [15,16]). Quite a few studies have attempted to compare directly combustion properties of DME and ethanol (e.g. [3,11]). In the study from Wang et al. [11] the authors compared extinction limits for pure DME and pure ethanol in non-premixed counter flow flames.

The aim of the current study was to contribute with experimental data from non-premixed flames of DME and ethanol and particularly, to elucidate their differences through a comparative study on critical conditions that lead to extinction and autoignition in such flames. The measurements were performed using the counter flow burner method. The examined fuels included not only the pure substances but also several blends of DME/ ethanol with different compositions.

Experimental Setup and Procedure

Figure 1 shows a schematic illustration of the experimental setup that consists of the counter flow burner, the fuel and oxidizer supply system, and the hardware/software used to control the experiment and to acquire the experimental data. As shown in the schematic drawing of the burner in Figure 2, fuel is injected from the lower duct, while the oxidizer is injected from the upper duct. The fuel and the oxidizer ducts are aligned concentrically and surrounded by annular ducts that provide a curtain flow of nitrogen to minimize the influence of ambient air on the reaction zone. Fine wire screens are placed at the exits of the two ducts in order to create plug flow conditions [17]. At the lower part of the burner, the fuel and curtain ducts are surrounded by another annular section, concentrically arranged around the curtain duct. A slight vacuum is applied in this section to drive the exhaust gas out of the burner. Water cooling is also applied in that same section to quench the reactivity of the exhaust gas before its disposal to the in-house exhaust system.

Corresponding author: alexandra.loukou@kit.edu

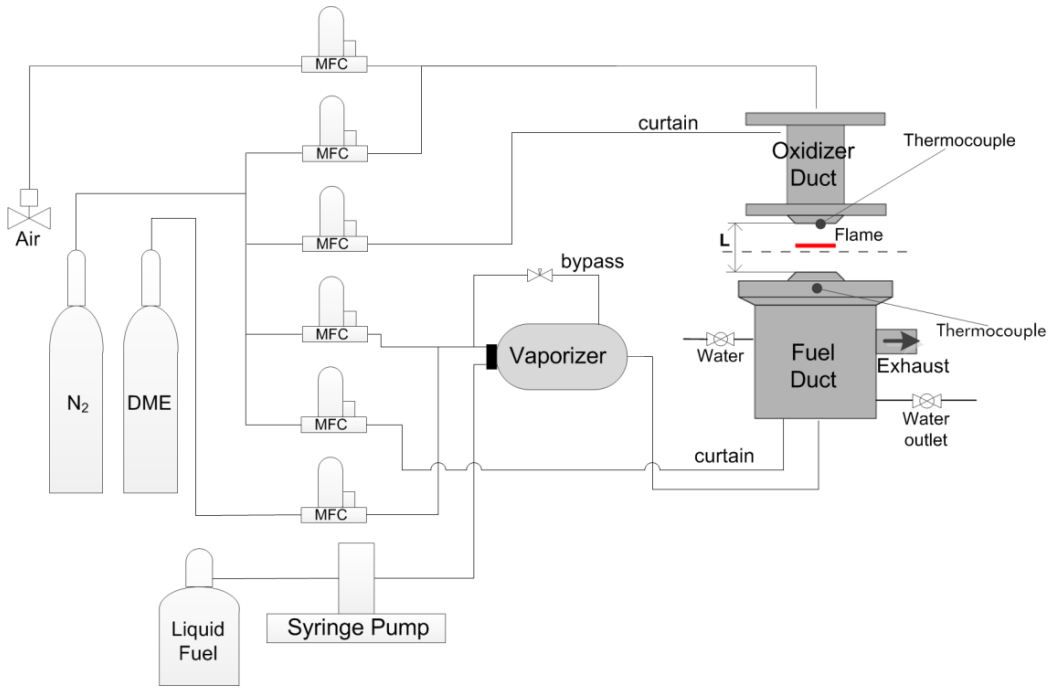

Figure 1: Schematic drawing of the experimental setup with the counter flow burner

With regard to the upper burner part, there are few differences between the basic design used for extinction experiments and the one used for investigating autoignition. In the case of extinction, the upper part has a simple design, consisting of two concentric tubes that separate the oxidizer gas from the curtain gas. For autoignition investigations, the upper part has still the same basic design employing additionally, a heating element out of SiC. The heating element is installed in the oxidizer duct, concentrically aligned with the later, and is used to preheat the oxidizer stream so as to reach the desired temperatures at the oxidizer boundary. The respective experimental procedure will be explained in the next sections. In general, the upper parts of the burner are exchangeable depending on the type of experiment. Further details about the design of the burner can be found in earlier studies by the group of Prof. Seshadri in University of California, San Diego, where it was initially developed (e.g. [17,18].)

The currently presented investigations were performed under atmospheric conditions and the fuel stream was supplied in gaseous form, containing DME, pre-vaporized ethanol and nitrogen. In order to create the mixture, nitrogen and DME were supplied out of high pressure bottles and their volume flows were regulated with the use of calibrated thermal mass flow controllers. The two gases were mixed before the addition of ethanol. Ethanol was supplied in liquid form with a syringe pump and then it was sprayed and vaporized within the vaporizer, using the DME/ nitrogen mixture as carrier gas. Downstream of the vaporizer, the fuel line was heated to avoid condensation of ethanol within the fuel stream. For the oxidizer stream, dry compressed air and bottled nitrogen were supplied with thermal mass flow controllers and were mixed before entering the upper part of the burner according to the desired experimental conditions.

It is important to introduce at this point a set of parameters that are used to describe thermodynamic and flow conditions when extinction and autoignition are investigated. This set of parameters includes the fuel mass fraction ($Y_{F,1}$), the temperature at the fuel boundary (T_1), the component of the flow velocity normal to the stagnation plane at the fuel boundary (V_1), the mass fraction of oxygen ($Y_{O2,2}$), the temperature at the oxidizer boundary (T_2), the component of the flow velocity normal to the stagnation plane at the oxidizer boundary (V_2) and finally the strain rate (a).

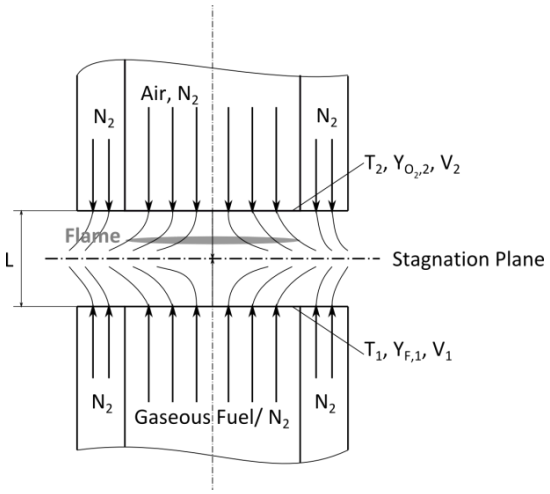

Figure 2: Schematic illustration of the counter flow configuration.

The mass fractions $Y_{F,1}$ and $Y_{O2,2}$ are important parameters as they define the stoichiometric mixture fraction and the position of the flame:

$$Z_{st} = 1 + \frac{vY_{F,1}}{Y_{O_2,2}} \tag{1}$$

where v is the stoichiometric oxygen-to-fuel mass ratio. The velocities V_1 and V_2 are presumed to be equal to the ratio of the respective volumetric flow rates to the cross-section area of the ducts. The temperatures T_1 and T_2 are measured with the use of thermocouples.

The strain rate, for this type of flow, it is defined as the normal gradient of the normal component of the flow velocity. The strain rate α_2 at the oxidizer stream can be estimated from equation (2) [19]. The derivation of the equation was explicitly presented in a recent publication from Niemann, Seshadri and Williams [17].

$$a_2 = 1 + \frac{2V_2}{L}\left(1 + \frac{V_1\sqrt{\rho_1}}{V_2\sqrt{\rho_2}}\right) \tag{2}$$

Here ρ_1 and ρ_2 represent the densities of the mixture at the fuel and oxidizer boundaries, respectively. The parameter L is the distance between the fuel boundary and the oxidizer boundary (Figure 2).

Momentum balance is imposed experimentally in order to keep the stagnation plane in the middle between the two ducts according to the following expression:

$$\rho_1 V_1^2 = \rho_2 V_2^2 \tag{3}$$

Combining equations (2) and (3), the strain rate α_2 can be written as:

$$\alpha_2 = \frac{4V_2}{L} \tag{4}$$

The last equation is particularly useful owing to the direct correlation of the strain rate with the two parameters V_2 and L, which can be easily controlled during experiments.

Critical Conditions of Extinction

Extinction experiments were conducted with a duct separation of L = 12.5 mm. The temperature at the fuel boundary was kept at T_1 = 400 K in order to avoid ethanol condensation and the temperature at the oxidizer boundary was T_2 = 298 K. The uncertainty of the temperature measurements is within ± 20°K. At a fixed fuel composition, fuel mass fraction and oxidizer mass fraction, the flame was stabilized at a strain rate (a_2) lower than the extinction strain rate. Following, the strain rate was increased stepwise until extinction was observed. The procedure was repeated varying systematically the compositions of the fuel (Y_{F1}, $Y_{DME,1}$, $Y_{eth,1}$) and the oxidizer stream ($Y_{O2,2}$), which were selected so as to keep the same stoichiometric mixture fraction, Z_{st} = 0.328 and adiabatic flame temperature, T_{ad} = 1900 K. According to the work of Kim and Williams [20], for fixed Z_{st} and T_{ad}, the scalar dissipation rate in the flame (x_{st}) is only dependent on the applied strain rate.

Due to the fact that the experiments were carried out with mixtures of DME and ethanol it is not trivial to calculate the mass fractions for given Z_{st} and T_{ad}. The group at UCSD developed an asymptotic formulation of the problem based on earlier studies (e.g.[21]) which enables the calculation of the parameters Y_{F1}, $Y_{DME,1}$, $Y_{eth,1}$ $Y_{O2,2}$ when Z_{st} and T_{ad} are known parameters. In this formulation it is assumed that the Damköhler numbers are high and the Lewis numbers for both fuels are 1.50.

The x_{st} is evaluated from:

$$Z_{st} = \frac{1}{2} erfc\left(x_{st}\sqrt{\frac{1}{2}}\right) \tag{5}$$

The stoichiometric mixture for ethanol and DME can be calculated as:

$$Z_{eth,st} = \frac{1}{2} erfc\left(x_{st}\sqrt{\frac{Le_{eth}}{2}}\right) \tag{6}$$

$$Z_{DME,st} = \frac{1}{2} erfc\left(x_{st}\sqrt{\frac{Le_{DME}}{2}}\right) \tag{7}$$

The mass fraction of ethanol and the mass fraction of oxygen can be obtained by choosing the mass fraction of DME and solving:

$$3g + 3m = c \tag{8}$$

with:

$$g = \frac{1}{\sqrt{Le_{eth}}} \frac{X_{eth,1}}{1 - Z_{eth,st}} \left(\exp\left(\frac{x_{st}^2(1 - Le_{eth})}{2}\right)\right) \tag{9}$$

$$g = \frac{1}{\sqrt{Le_{DME}}} \frac{X_{DME,1}}{1 - Z_{DME,st}} \left(\exp\left(\frac{x_{st}^2(1 - Le_{DME})}{2}\right)\right) \tag{10}$$

$$c = \frac{X_{O_2,2}}{Z_{st}} \tag{11}$$

$$T_{ad} = T_u + \frac{1}{c_p W_{N_2}}\left(Q_{eth} g + Q_{DME} m\right) Z_{st}(1 - Z_{st}) \tag{12}$$

with $x_{eth,1} = \frac{Y_{eth,1} W_{N_2}}{W_{C_2H_6O}}$; $x_{DME,1} = \frac{Y_{DME,1} W_{N_2}}{W_{C_2H_6O}}$;

$$x_{eth,1} = \frac{Y_{O_2,2} W_{N_2}}{W_{O_2}} \tag{13}$$

In equation (12) Q_{DME} is the heat release of DME (1328×10^3 J/mol), Q_{eth} the heat release of ethanol (1278×10^3 J/mol), c_p the heat capacity (1300 J/kgK), W_{O2} the molecular weight of oxygen, W_{N2} the molecular weight of oxygen and W_{C2H6O} the molecular weight of DME and ethanol. Equations (8) – (13) were solved iteratively, varying $Y_{DME,1}$ from 0 to 1. The solutions

that were obtained are summarized in Table 2 and were applied when conducting the extinction experiments.

Table 2: Composition of fuel and oxidizer stream during extinction experiments

	$Y_{O2,2}$	$Y_{DME,1}$	$Y_{eth,1}$	$Y_{F,1}$	$Y_{N2,1}$
1	0.2330	0.00	0.3105	0.3105	0.6895
2	0.2325	0.02	0.2897	0.3097	0.6903
3	0.2319	0.04	0.2689	0.3089	0.6911
4	0.2313	0.06	0.2481	0.3081	0.6919
5	0.2307	0.08	0.2273	0.3073	0.6927
6	0.2301	0.10	0.2065	0.3065	0.6935
7	0.2296	0.12	0.1858	0.3058	0.6942
8	0.2290	0.14	0.1650	0.3050	0.6950
9	0.2284	0.16	0.1442	0.3042	0.6958
10	0.2278	0.18	0.1234	0.3034	0.6966
11	0.2272	0.20	0.1026	0.3026	0.6974
12	0.2266	0.22	0.0818	0.3018	0.6982
13	0.2260	0.24	0.0610	0.3010	0.6990
14	0.2255	0.26	0.0403	0.3003	0.6997
15	0.2249	0.28	0.0195	0.2995	0.7005
16	0.2243	0.30	0.0000	0.2980	0.7020

The strain rate at extinction, $a_{2,e}$ was recorded as function of composition of the DME/ ethanol blend. The accuracy of the strain rate is ± 10% of recorded value and that of the fuel mass fraction ± 3% of recorded value. The experimental repeatability on reported strain rate is ± 5% of recorded value. Figure 3 shows the respective data. It can be observed that as the DME content of the blends increase the flames become more difficult to extinguish.

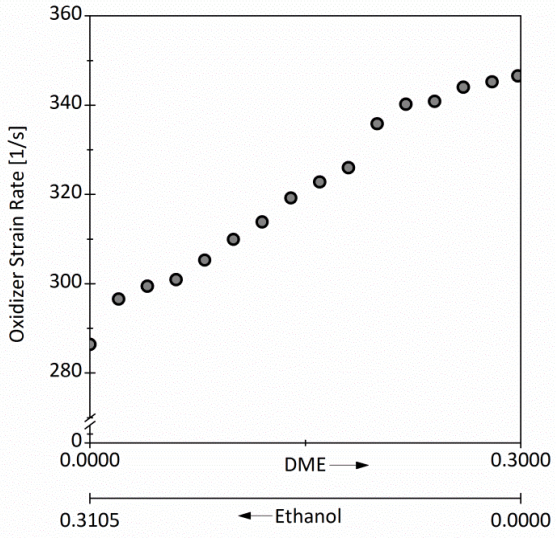

Figure 3: Oxidizer extinction strain rates as a function of the composition of the DME/ ethanol blend.

Critical Conditions of Autoignition

Ignition experiments were carried out with a duct separation of L = 14.5 mm, fuel stream exit temperature of 400 K (± 20 K) and fuel mass fraction of $Y_{F,1}$ = 0.40. The oxidizer stream was air so the mass fraction of oxygen was $Y_{O2,2}$ = 0.233. At a fixed strain rate a_2, the temperature at the oxidizer boundary T_2 was increased until autoignition took place. The velocities of the counter flowing streams were constantly adjusted based on the temperature change in order to maintain balanced momenta. The value of T_2 at autoignition ($T_{2,i}$) is considered as the autoignition temperature. A high-speed CCD camera was used to observe the onset of ignition at a frame rate of 500 s^{-1}. Temperature data were recorded only for cases where autoignition was observed to occur close to the axis of symmetry. The procedure was repeated for different compositions of DME/ ethanol blends and for different values of strain rate a_2.

The thermocouple employed for measuring the temperature T_2 during the experiment is an R-type thermocouple (Pt/13%Rh-Pt) with a wire diameter of 76 µm and bead size of 210 µm. The thermocouple was placed at the exit of the oxidizer duct. The temperature values presented in the following graphs are the arithmetic means of three samples taken for each set of examined conditions. The total uncertainty of the measurements lies within ± 50 K and has been estimated taking into account the intrinsic accuracy of R-type thermocouples, radiative and convective losses from the thermocouple bead and the deviation from the mean value in each sample.

While the fuel mass fraction $Y_{F,1}$ was kept constant in these experiments, different compositions of DME/ ethanol blends were tested, starting with pure ethanol and increasing the mole fraction of DME in the mixture in steps of 0.20 up to 100% DME. The tested blends are presented in Table 3.

Table 3: Composition of fuel stream during autoignition experiments

	X_{eth}	X_{DME}
1	1.00	0.00
2	0.80	0.20
3	0.60	0.40
4	0.50	0.50
5	0.40	0.60
6	0.20	0.80
7	0.00	1.00

Figure 4 shows the autoignition temperature of different DME/ ethanol blends over the oxidizer strain rate. Among all tested fuels, it is found that ethanol has the lowest autoignition temperature at all strain rates. It seems that an increase of the DME content in the fuel mixture leads to an increase of the autoignition temperature and the effect appears to be uniform, independent of the strain rate.

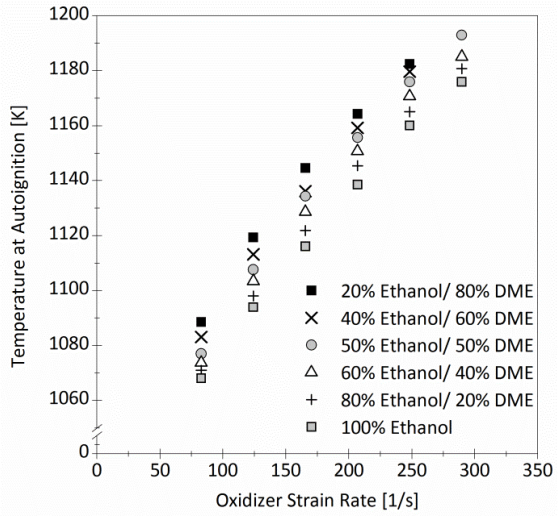

Figure 4: The temperature at autoignition of the oxidizer stream as a function of the oxidizer strain rate at a constant fuel mass fraction of $Y_{F,1} = 0.40$. The figure shows data for blends of DME/ethanol with ethanol content ranging from 20% up to 100%.

Figure 5 compares the temperature at autoignition for pure DME, pure ethanol and the blend with 20% ethanol/ 80% DME. Taking into account the data shown in Figure 4, one would expect that that a further increase of the DME content up to 100% would shift the autoignition temperature even higher compared to the 20% ethanol/ 80% DME. However, the measurements reveal the opposite and $T_{2,i}$ for pure DME lies for all strain rates between $T_{2,i}$ for the 20% ethanol/ 80% DME blend and $T_{2,i}$ for pure ethanol.

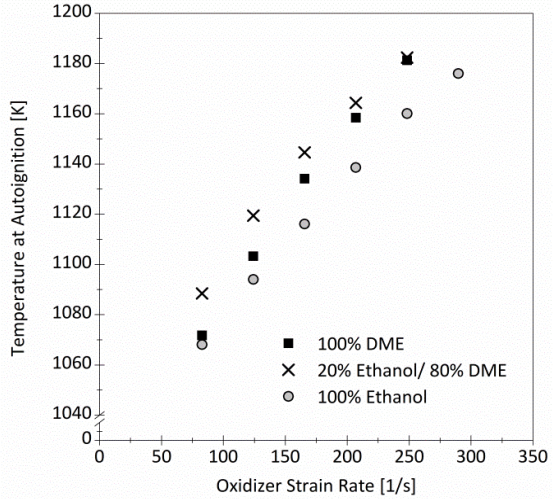

Figure 5: The temperature at autoignition of the oxidizer stream as a function of the oxidizer strain rate at a constant fuel mass fraction of $Y_{F,1} = 0.40$. The figure shows data for pure ethanol, pure DME and the blend 20%ethanol/80%DME.

While pure DME exhibits higher autoignition temperatures compared to pure ethanol, the gradient $dT_{2,i}/da_2$ is a lot steeper for pure DME. It can also be observed that the autoignition temperature of pure DME at an oxidizer strain rate $a_2 = 82.78$ 1/s is almost equal to that of pure ethanol (only 4 K higher compared to pure ethanol). With an addition of 20% ethanol in DME, the autoignition temperature at the same strain rate increases for about 20 K.

By plotting the oxidizer temperature at autoignition over the composition of the examined DME/ ethanol blends the obtained results can be observed in a different way. As shown in Figure 6, of all fuels tested in this study, the blend with 20% ethanol/ 80% DME exhibits the highest autoignition temperature. Compared to pure DME, it can also be seen that the addition of 20% ethanol raises $T_{2,i}$ but the effect gets limited at very high strain rates. In particular, the increase in $T_{2,i}$ at a strain rate $a_2 = 82.78$ 1/s is $\Delta T_{2,i} = 17$ K, while at the highest strain rate $a_2 = 248.28$ 1/s there is almost no increase ($\Delta T_{2,i} = 1$ K).

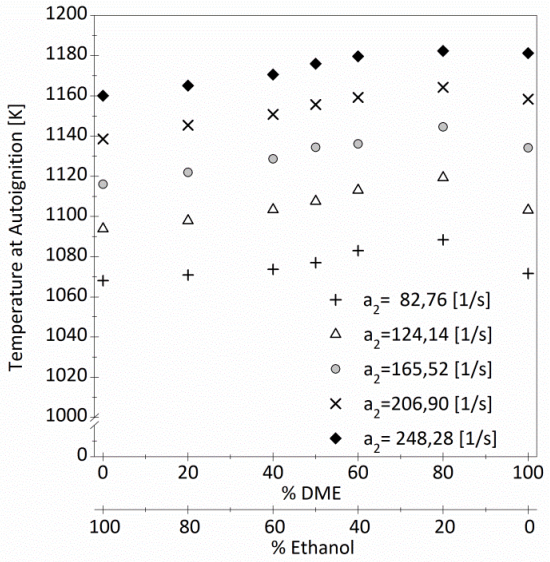

Figure 6: The temperature at autoignition of the oxidizer stream as a function of the composition of the DME and ethanol blend at a constant fuel mass fraction of $Y_{F,1} = 0.40$. The figure shows data at different oxidizer strain rates.

Conclusions

The main focus of this experimental study was to determine how DME and ethanol influence each other in terms of extinction and autoignition limits in non-premixed flames. Critical conditions of extinction and autoignition were measured for non-premixed flames stabilized in a counter flow burner.

The critical conditions of extinction were measured with the mass fractions of the opposing streams chosen at a fixed adiabatic flame temperature and stoichiometric mixture fraction in order to isolate chemical effects from fuel property effects. The strain rate at extinction was found to increase with increasing amounts of DME in the combustible mixture.

At low strain rates, the autoignition temperature of DME was nearly the same as for ethanol. By mixing ethanol and DME, the autoignition temperature was found to increase, exhibiting a peek for the 20% ethanol/ 80% DME blend. At higher strain rates, this effect was less pronounced and vanished by further increasing the strain rate. At low strain rates, the

ignition of DME appears to be influenced by the low temperature chemistry.

The current results show that in mixtures of DME and ethanol, autoignition as well as extinction is delayed with increasing amounts of DME.

Acknowledgments

The authors would like to acknowledge the financial support by the Saxonian Ministry of Science and Fine Arts and the European Union in the project "DynMo" (100113147). The authors would also like to acknowledge the financial support by the Marshall Plan Foundation.

References

[1] M. Balat, H. Balat, C. Öz, Prog. Energy Combust. Sci. 34 (2008) 551–573.

[2] E.W. Kaiser, T.J. Wallington, M.D. Hurley, J. Platz, H.J. Curran, W.J. Pitz, C.K. Westbrook, J. Phys. Chem. A 104 (2000) 8194–8206.

[3] C.S. McEnally, L.D. Pfefferle, Proc. Combust. Inst. 31 (2007) 603–610.

[4] F. Rau, S. Hartl, S. Voss, M. Still, C. Hasse, D. Trimis, Fuel 140 (2015) 10–16.

[5] J.P.J. van Lipzig, E.J.K. Nilsson, L.P.H. de Goey, A.A. Konnov, Fuel 90 (2011) 2773–2781.

[6] D. Bradley, M. Lawes, S. Liao, A. Saat, Combust. Flame 161 (2014) 1620–1632.

[7] J. Beeckmann, L. Cai, H. Pitsch, Fuel 117 (2014) 340–350.

[8] M. Salamanca, M. Sirignano, A. D'Anna, Energy & Fuels 26 (2012) 6144–6152.

[9] R. Seiser, S. Humer, K. Seshadri, E. Pucher, Proc. Combust. Inst. 31 (2007) 1173–1180.

[10] P. Saxena, F.A. Williams, Proc. Combust. Inst. 31 (2007) 1149–1156.

[11] Y.L. Wang, P.S. Veloo, F.N. Egolfopoulos, T.T. Tsotsis, Proc. Combust. Inst. 33 (2011) 1003–1010.

[12] C.A. Daly, J.M. Simmie, J. Wu, 2180 (2001).

[13] Z. Chen, C. Tang, J. Fu, X. Jiang, Q. Li, L. Wei, Z. Huang, Fuel 102 (2012) 567–573.

[14] X. Qin, Y. Ju, Proc. Combust. Inst. 30 (2005) 233–240.

[15] S. Deng, P. Zhao, D. Zhu, C.K. Law, Combust. Flame (2014) 1–5.

[16] F. Herrmann, P. Oßwald, K. Kohse-Höinghaus, Proc. Combust. Inst. 34 (2013) 771–778.

[17] U. Niemann, K. Seshadri, F.A. Williams, Combust. Flame (2014).

[18] R. Seiser, K. Seshadri, E. Piskernik, A. Liñán, Combust. Flame 122 (2000) 339–349.

[19] K. Seshadri, F.A. Williams, Int. J. Heat Mass Transf. 21 (1978) 251–253.

[20] J.S. Kim, F.A. Williams, SIAM J. Appl. Math. 53 (1993) 1551–1566.

[21] R. Seiser, L. Truett, K. Seshadri, Proc. Combust. Inst. 29 (2002) 1551–1557.